


ORIGINAL ARTICLE

Vascularized composite allotransplants as a mechanistic model for allograft rejection – an experimental study

Dimitrios Moris¹ , Jun Wang¹, Maria Angelica Selim², Mingqing Song¹ , Linda Stempora¹, William Parker¹, Allan D. Kirk¹ & Linda C. Cendales¹ 

¹ Department of Surgery, Duke University Medical Center, Durham, NC, USA

² Department of Pathology, Duke University, Durham, NC, USA

Correspondence

Linda C. Cendales, Duke Vascularized Composite Allotransplantation Program, Duke University Medical Center, 129 Baker House, Durham, NC 27710, USA.

Tel.: + 919-6817514;

fax: + 919-684-2670;

e-mail: linda.cendales@duke.edu

SUMMARY

Vascularized composite allotransplants (VCAs) seem to have several unique features of clinical and experimental importance, including uniquely definable lymphatic drainage that can be easily accessed at the level of ipsilateral regional node beds. Thus, VCA offers a unique opportunity to assess the relative contribution of peripheral and secondary lymphoid tissue to the process of rejection. We transplanted hind limb grafts from C3H donors to six different groups of C57BL/6 recipients: Spleen⁺Map3k14^{-/-}; Spleen⁻Map3k14^{-/-}; Spleen⁺Node⁻Map3k14^{-/-}; and Spleen⁻Node⁻Map3k14^{-/-}. As positive controls, we used Map3k14^{+/-} with or without spleen. Map3k14^{+/-} mice demonstrated an average graft survival of 9.6 and 9.2 days for Spleen⁻ and Spleen⁺Map3k14^{+/-}, respectively. Rejection in the Map3k14^{-/-} group was considerably delayed (28.4 days, $P = 0.002$) in all recipients. The Spleen⁻Map3k14^{-/-} mice rejected their hind limb allografts in an even more delayed fashion compared to Spleen⁺Map3k14^{-/-} (54.4 days, $P = 0.02$). Histological analysis of skin showed that acute rejection in both Map3k14^{+/-} mice groups was graded as Banff III or Banff IV. In the Map3k14^{-/-} groups, rejection was graded as Banff III. We demonstrated that in the absence of lymph nodes, grafts reject in a delayed fashion. Also, splenectomy in alymphoplastic mice further extends graft survival, but does not eliminate rejection all together.

Transplant International 2021; 34: 572–584

Key words

acute rejection, hind limb, secondary lymphoid organs, vascularized composite allotransplantation

Received: 23 October 2020; Revision requested: 9 December 2020; Accepted: 11 January 2021;

Published online: 9 February 2021

Introduction

Vascularized composite allotransplants (VCAs) have emerged as means of restoring form and function for selected individuals following devastating injury or limb loss [1]. As with other solid organ grafts, they are limited by immune-mediated rejection and a concomitant requirement for immunosuppression [2,3]. Although VCA rejection is assumed to be mechanistically similar

to the rejection of other organs, several unique features of VCAs are notable from an experimental perspective. For example, VCAs are uniquely accessible for direct observation and serial biopsy. Their vascular drainage is similar to other organs, though VCAs, particularly limb transplants, have uniquely definable lymphatic drainage via a series of deep and superficial channels that regenerate and ultimately drain into the easily accessible ipsilateral node beds [4]. Additionally, most VCAs contain

donor-derived lymph nodes. Thus, VCAs offer a unique opportunity to assess the relative contribution of peripheral and secondary lymphoid tissue to the process of rejection—both that of VCAs and perhaps more generally.

Physiologic adaptive immune responses are most effectively initiated in secondary lymphoid organs (spleen and lymph nodes), with effector responses returning to the site of antigen burden to mediate antigen clearance [5,6]. This standard paradigm is often evoked for allografts, though numerous differences likely alter the origin and maintenance of alloimmune responses relative to protective immune responses. These include direct recognition of widely distributed donor MHC molecules on passenger leukocytes. These, combined with ubiquitous reperfusion events, plausibly allow for peripheral antigen presentation by activated non-professional antigen-presenting cells (APCs) such as vascular endothelium [7,8]. Additionally, heterologous immunity provides mechanisms by which cells primed via prior conventional protective immune mechanisms can undergo anamnestic activation to novel alloantigens without the need for a *de novo* priming event. The precursor frequency to allografts is also log-fold greater than that to environmental pathogens [9], making even inefficient means of cell activation potentially effective in mustering a detrimental immune response. Thus, the relative, and likely non-exclusive, contributions of formal priming in secondary lymphoid tissues versus peripheral mechanisms of priming or recruitment of heterologous immune memory remain incompletely established for all allografts, with the unique anatomic properties of VCAs being uniquely exploitable for exploration of these fundamental tenets.

In this work, we have adopted a recently established mouse hind limb transplant model [10] to highlight the utility of VCAs in mechanistic exploration. We go on to demonstrate that in the absence of lymph nodes, limb grafts reject in a delayed fashion. Also, splenectomy in alymphoplastic mice further extends graft survival, but does not eliminate rejection all together. We posit that the capacity to isolate these peripheral and central modes of allosensitization will have utility in a reductionist approach to studying primarily vascularized organ allografts.

Materials and methods

Mice and hind limb transplantation

All hind limb donors were 6- to 8-week-old C3H (H-2^k) male mice, and all recipients were 6- to 8-week-old

male mice of the C57BL/6 (H-2^b) background. To determine whether secondary lymphoid organs are essential for initiating the alloimmune response to VCAs, we transplanted hind limb grafts from C3H donors to six different groups of C57BL/6 recipients: non-splenectomized alymphoplastic (Spleen⁺Map3k14^{-/-}) mice; splenectomized alymphoplastic (Spleen⁻Map3k14^{-/-}) mice; non-splenectomized alymphoplastic without regional (inguinal and popliteal) nodes (Spleen⁺Node⁻Map3k14^{-/-}); and splenectomized alymphoplastic without regional nodes (Spleen⁻Node⁻Map3k14^{-/-}). As positive controls, we used heterozygous C57BL/6 recipients (Map3k14^{+/-}) with or without spleen, which have normal secondary lymphoid organs. Wild-type C57BL/6 recipients were used as syngeneic (negative) controls.

MAP3K14 also known as NIK (NF- κ B inducing kinase) mediates development and architectural organization of secondary lymphoid organs. Point mutation causes alymphoplastic phenotype and homozygotes present with abnormal lymphorganogenesis, devoid of lymph nodes and Peyer's patches, abnormal spleen/thymus morphology, near-normal T-cell levels, and drastically reduced B cells [11–13].

Mice weighing 20–25 g were used for the experiment. Mice were purchased from the Jackson Laboratories (Bar Harbor, ME, USA). Animals were housed and fed ad libitum at Duke University Medical Center (Durham, NC, USA) following the institutional guidelines for the appropriate care and use of laboratory animals. The experiments described in this study were approved by the Institutional Animal Care and Use Committee at Duke University.

Hind limb transplantation was performed as previously described [10]. Five animals per group were included in the analysis. In the Spleen⁻ group, splenectomy was performed 2 weeks before hind limb transplantation. Briefly, at the time of hind limb transplantation, we collected the donor spleen (if Spleen⁺) and the contralateral inguinal node. After removal of the recipient limb, we also collected the recipient inguinal node from that limb as a baseline (if the recipient was Map3k14^{+/-}). The hind limb graft was transplanted with the donor inguinal node within the graft (with the exceptions of the groups that were node negative; Fig. 1a,b). For hind limb node mapping, we injected 50 μ l of methylene blue in the graft foot pad with a 30-gauge needle syringe. Popliteal and inguinal nodes were identified visually and removed before graft removal and transplantation (Fig. S1).

The mice were monitored daily, and the grafts were evaluated for visual signs of acute rejection including

erythema and rash. Animals were euthanized when developing persistent or progressive skin lesions (rejection) or at 90 days post-transplant. At the time of euthanasia, the recipient spleen and the inguinal node contralateral to the graft are removed if present. The draining allograft lymph node is also collected (Fig. 1c). Tissues were analyzed using histology and flow cytometry.

Flow cytometry

All antibodies were purchased commercially and tested for optimal dilution in-house, based on lot, clone, and vendor. In general, single cell suspensions were isolated from blood, inguinal lymph node, and spleen. After red cells were lysed, approximately 1×10^6 cells were transferred to wells of a round bottom 96-well plate. Cells were incubated with a fixable live/dead stain for 30 min, washed, and then stained with the surface antibodies cocktails listed in Table S1. After incubating for 30 minutes, cells were either washed and fixed for flow analysis or they were stained for intracellular markers using the BD Cytofix/Perm buffer kit. Cells were washed and resuspended in staining buffer for flow analysis. Data were collected using a BD Fortessa X20 instrument running BD FACS DIVA software version 8.0.1. Data were analyzed using FlowJo™ Software (for Mac) FlowJo version 9.9.6 (Ashland, OR, USA; Fig. S2).

In mice, CD4 and CD8 T cells can be further categorized into memory and naïve phenotypes based on CD62L (L-selectin) and CD44 expression with the CD44⁻CD62L⁺ population considered naïve, CD44⁺CD62L⁺ population considered central memory, and the CD44⁺CD62L⁻ population considered effector and/or effector memory. It is known that CD4 and CD8

T cells differ in their distribution of these subsets in lymphoid and peripheral organs. While naïve frequencies within CD4 and CD8 populations remain relatively similar, the CD44⁺ population is more central memory skewed in CD8 T cells and effector memory skewed in CD4 T cells in a resting organism [14].

Statistical analysis

Statistical analysis was performed using PRISM software (GraphPad Software Inc., San Diego, CA, USA). Data were expressed as mean \pm SEM. For analysis of three or more groups, the nonparametric one- or two-way ANOVA test (where appropriate) was performed with the Bonferroni post-test. Analysis of differences between two normally distributed test groups was performed using Student's *t*-test. Welch's correction was applied to Student's *t*-test data sets with significant differences in variance. **P* < 0.05, ***P* < 0.01, and ns: *P* > 0.05.

Histology

A skin biopsy was taken at the time of euthanasia and fixed in 10% neutral-buffered formalin then embedded in paraffin. The paraffin sections were cut at 5 μ m and stained with hematoxylin and eosin (H&E) to visualize the graft morphology and cellular infiltration.

Whole stained slides were scanned with the Aperio Scanscope AT Turbo digital slide scanner system (Leica Biosystems, Vista, CA, USA) and viewed with Aperio Imagescope digital pathology software (Leica Biosystems) by a dermatopathologist who was blinded to the recipients' phenotypes. The samples are reviewed and scored for acute allograft rejection according to the Banff 2007 working classification of skin-containing composite tissue allograft pathology [15].

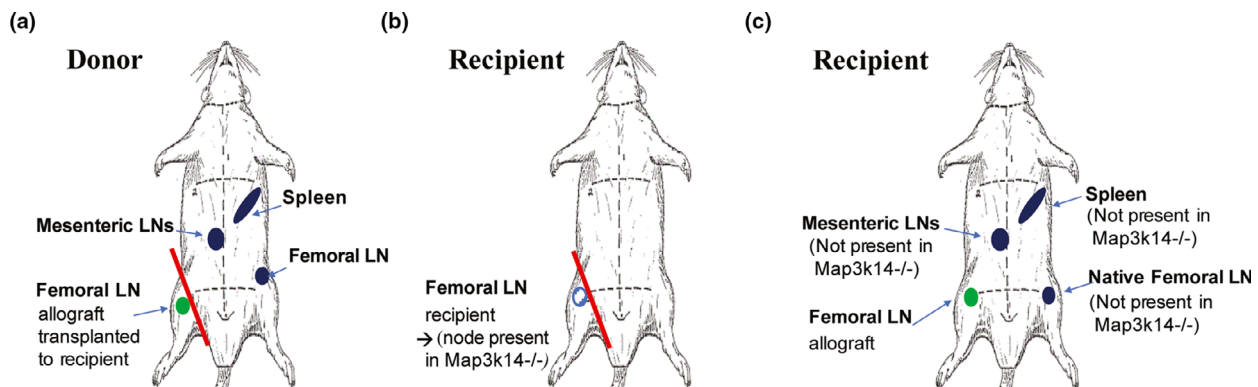


Figure 1 Tissue procurement at the time of hind limb transplant in the donor (a) and recipient (b). Tissue procurement at the time of sacrifice (c).

Results

Lack of secondary lymphoid tissue confers a survival advantage in hind limb transplantation

Visually, skin changes occurred in all except in one animal. Map3k14^{+/-} (phenotypically normal and heterozygote controls) mice rejected hind limb allografts, with an average graft survival of 9.6 and 9.2 days for Spleen⁻ and Spleen⁺Map3k14^{+/-}, respectively (Fig. 2a,b). Rejection in the Map3k14^{-/-} (phenotypically alymphoplastic) group was considerably delayed (average graft survival: 28.4 days, $P = 0.002$) in all recipients (Fig. 2c). The splenectomized Map3k14^{-/-} mice rejected their hind limb allografts in an even more delayed fashion compared to Spleen⁺Map3k14^{-/-} (Fig. 2d) and one animal that did not reject (Fig. S3a) during the 90-day experimental follow-up (average graft survival: 54.4 days, $P = 0.02$). Allografts in which the donor lymph nodes were removed at the time of transplantation were all rejected at similar tempo with the grafts with regional nodes (average graft survival 45 and 30.5 for Spleen⁻Node⁻Map3k14^{-/-} and Spleen⁺Node⁻Map3k14^{-/-} grafts, respectively; Fig. 2e,f). All syngeneic mice reached the endpoint of 90 days without any signs of acute rejection (Fig. 2g). Histological analysis of skin showed that acute rejection in both Map3k14^{+/-} mice groups was graded as Banff III or Banff IV (Fig. 2a,b). In the Map3k14^{-/-} groups, rejection was graded as Banff III (Fig. 2c,d). The skin biopsy of the Spleen⁻Map3k14^{-/-} animal that did not have visual signs of rejection and was graded as Banff 0 at sacrifice (Fig. S3b). In the donor node⁻ groups, acute rejection was graded as Banff III (Fig. 2e,f). However, two Spleen⁻Node⁻Map3k14^{-/-} that developed persistent skin lesions, the histology revealed neutrophil infiltrates without lymphocytes or distortion of the normal anatomy (Banff 0). Skin from syngeneic mice at endpoint showed no rejection (Banff 0; Fig. 2g). Figure 3 summarizes the graft survival curves among all groups.

Lymph nodes and spleen T-cell populations

After hind limb transplantation, T-cell memory phenotypes varied in both CD8 and CD4 T cells in the inguinal nodes. In the syngeneic group, despite no changes in the percentages of CD3, CD4, and CD8 cells at the endpoint compared to baseline, there was a significant decrease of naïve as well as an increase in effector memory CD4 T cells in both graft and contralateral inguinal nodes. Similarly, an increase in the percentage of

effector CD8 cells was noted (Fig. 4). In the allogeneic groups, similar trends were noted in the graft nodes at the time of rejection that were more profound in the Map3k14^{-/-} groups (Fig. 5).

In the spleen of syngeneic mice at the endpoint, there was a significant decrease in naïve with a concomitant increase of effector memory CD4 and CD8 T cells (Fig. 6). On the contrary, in the acutely rejecting Map3k14^{+/-} mice there was an increase of both CD4 and CD8 naïve cells accompanied by a decrease of central and effector memory CD4 cells. The latter trend was reversed in the CD8 cell subset (Fig. 7). In the Map3k14^{-/-} group, a decrease in naïve as well as an increase in effector T cells was noted (Fig. 8). In the peripheral blood, there was no difference in CD3, CD4, and CD8 cells among all groups (Fig. S4).

Discussion

In this study, we found that in the absence of systemic lymph nodes, allogeneic hind limb grafts reject in delayed fashion and that splenectomy in the setting of absent lymph nodes further adds to graft survival without eliminating rejection altogether. The capacity to isolate these peripheral and central modes of allosensitization can facilitate and trigger further experiments in VCA focusing on the manipulation of regional lymphatics and its effect on allograft outcomes. The latter is a subject of ongoing research in the field [16,17]. Several studies have demonstrated the critical nature of secondary lymphoid organs in organ allograft rejection. Larsen et al first demonstrated in a mouse heterotopic heart transplant model that graft-derived APCs traffic to the spleen and that this is necessary for the development of an alloimmune response [18,19]. Lakkis *et al.* [20] examined immunologic “ignorance” of a vascularized graft in the setting of splenectomized, conditional knockout mice that lacked all secondary lymphoid structures. These insights triggered substantial investigation of pharmacologic strategies to modulate lymphocyte trafficking in the setting of transplantation [21].

Similarly, mice without secondary lymphoid organs demonstrated an impaired immune response to allogeneic intestines [22]. On the contrary, Gelman et al. showed that alloreactive T cells that are initially primed within lung allografts rather than in secondary lymphoid organs following transplantation lead to acute allograft rejection in the absence of secondary lymphoid organs [23]. Finally, mice lacking lymphatics acutely rejected allogeneic skin and heart grafts. In the absence of spleen, skin allografts were still rejected but cardiac

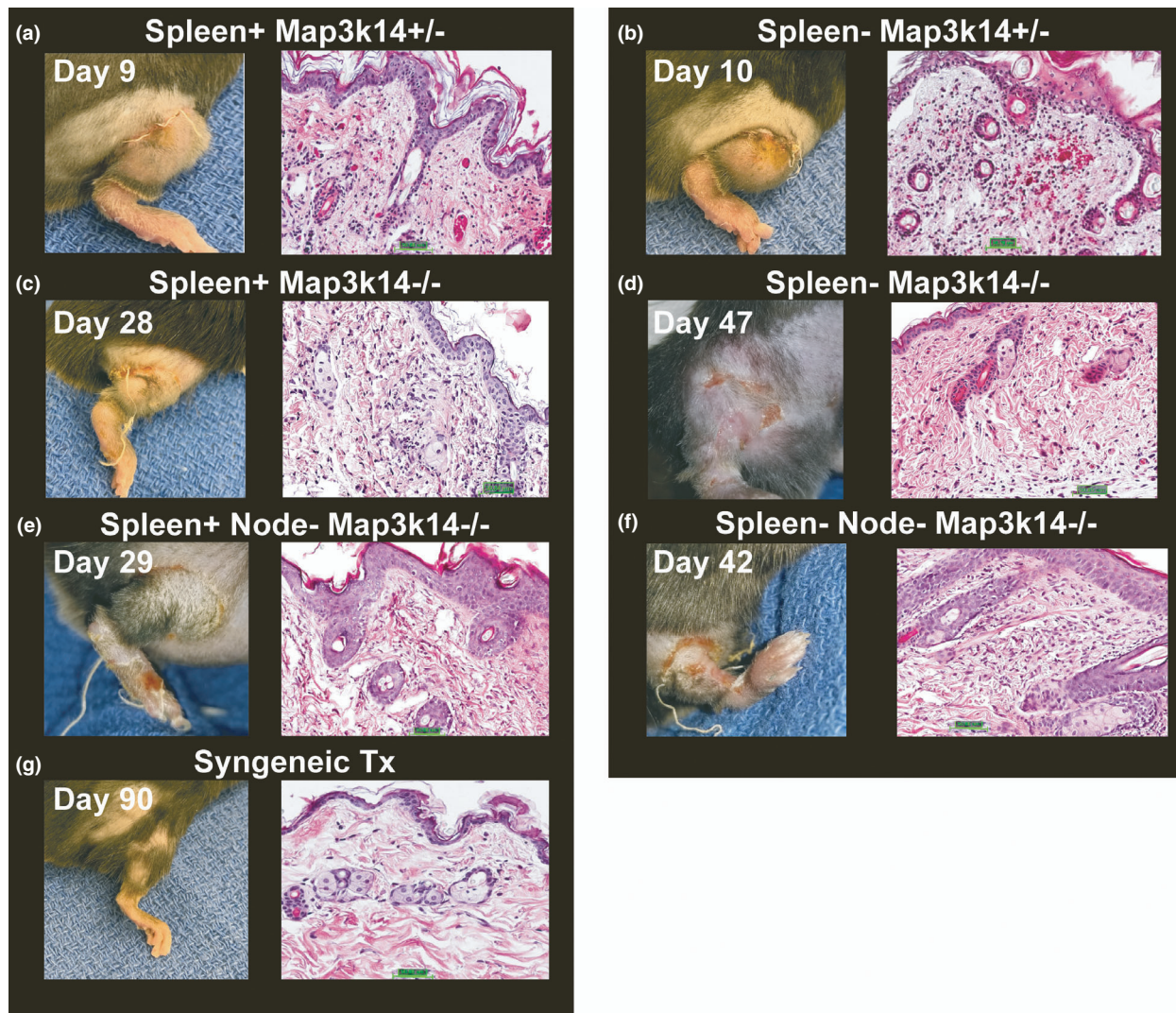


Figure 2 Clinical and histologic presentation at the time of sacrifice in all groups. (a) Spleen⁺Map3k14^{+/-} showing visual signs of acute rejection, including redness involving the graft and sparing the native skin. H&E-stained section showing detached epidermis associated with lymphocytic infiltrate admixed with neutrophils. (b) Spleen⁻Map3k14^{+/-} showing visual signs of acute rejection. H&E-stained section showing epidermis with isolated dyskeratotic cells and dermal lymphocytic infiltrate. (c) Spleen⁺Map3k14^{-/-} showing signs of acute rejection, including redness involving the graft and sparing the native skin and skin breakdown. H&E-stained section showing epidermis with dyskeratotic cells and dermal lymphocytic infiltrate. (d) Spleen⁻Map3k14^{-/-} showing signs of acute rejection, including epidermolysis involving the graft and sparing the native skin. H&E-stained section showing dermal mild edema and few lymphocytes (e) Spleen⁺Node⁻Map3k14^{-/-} showing signs of acute rejection, including epidermolysis involving the graft and sparing the native skin. H&E-stained section showing dermis with lymphocytic infiltrate. (f) Spleen⁻Node⁻Map3k14^{-/-} showing signs of acute rejection, including epidermolysis involving the graft and sparing the native skin. H&E-stained section showing acute rejection graded as BANFF III. (g) Syngeneic group showing no signs of acute rejection, hair regeneration and appropriate wound healing. H&E-stained section showing no acute rejection graded as BANFF 0.

transplants were not rejected. These findings indicate that in the absence of secondary lymphoid tissue, both rejection and tolerance of vascularized grafts are possible [24]. Similar to our study, all these experimental studies used Map3k14^{-/-} mice on B6 background as recipients of vascularized organs, facilitating the comparability of the results among studies. The advantage of Map3k14^{-/-} mouse model is that it lacks secondary

lymphoid organs but the number and function of peripheral T cells are normal. This allows the design of experimental studies evaluating the role of local immune responses in acute rejection of vascularized organs as well as the characterization of phenotype of lymphocytes contributing to achievement of tolerance (or delayed rejection). Especially in our model, this is of paramount importance since we were able to shed some

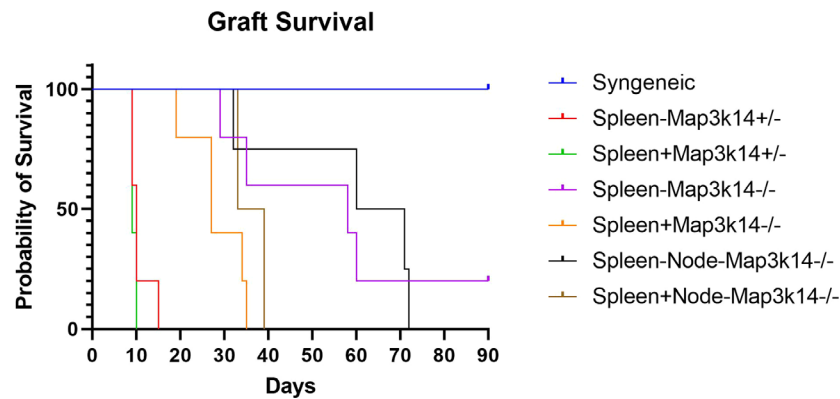


Figure 3 Graft survival among all groups. The average graft survival for Map3k14^{+/-} groups was 9.6 for the splenectomized and 9.2 days for the non-splenectomized mice. Acute rejection in the Spleen⁺Map3k14^{-/-} group was considerably delayed compared to Map3k14^{+/-} with and average graft survival of 28.4 days ($P = 0.002$). The Spleen-Map3k14^{-/-} mice rejected their hind limb allografts in even more delayed fashion compared to Spleen⁺Map3k14^{-/-}, with and average graft survival of 54.4 days ($P = .02$). Finally, node negative grafts were all rejected at similar tempo with the grafts with regional nodes (average graft survival 45 and 30.5 for Spleen⁻Node⁻Map3k14^{-/-} and Spleen⁺Node⁻Map3k14^{-/-} grafts respectively, $P = NS$). All syngeneic mice reached the endpoint of 90 days without any signs of acute rejection.

light on the role of regional lymph nodes in allograft immune response.

Efficient antigen presentation by way of secondary lymphoid structures provides ideal conditions for the timely development of an alloimmune response. Manipulation of access to this ideal environment could be anticipated to augment contemporary immunosuppressive strategies since the development of any de novo response to antigen requires the physical colocalization of APCs and lymphocytes. This occurs most efficiently in secondary lymphoid structures, where APCs organize and lymphocytes traffic and concentrate [25,26]. Mulvihill et al recently demonstrated that the addition of splenectomy and efferent lymphatic ligation to costimulation blockade-based immunotherapy decreases the rate of costimulation blockade-resistant rejection in non-human primates and improves rejection-free survival on belatacept monotherapy [27]. This observation is consistent with the prevailing understanding of costimulation molecules, specifically, that they facilitate antigen presentation, and with the premise that antigen presentation following a primarily vascularized allograft occurs in secondary lymphoid structures, including the spleen [18,28].

The mechanisms of skin rejection in VCA remain incompletely understood. There is an emerging literature on the formation of tertiary lymphoid organs (TLOs) in the setting of VCA rejection. These lymphoid organs can be found in the skin of different species such as humans, non-human primates, and rats and contain high numbers of B and T cells, especially memory subsets [29,30]. The variation in the number and activity of these entities might explain the differences in magnitude of rejection in

skin-containing VCAs. Besides the circulating T cells or those from lymphoid sites, vast numbers of T cells reside in multiple peripheral tissue sites including lungs, intestines, liver, and skin as non-circulating, tissue-resident memory T cells (Trm cells). Their role in VCA is not elucidated and given the growing reports of their presence in skin and contribution to autoimmune skin disease, their evaluation in allotransplantation seems relevant. It seems that the local cytokine milieu within tissue grafts promotes differentiation of infiltrating T cells into Trm. Also, if stimulated, Trm can initiate a series of immune-activating events commonly referred to as “sensing and alarm” function that leads to recruitment of circulating memory T cells and B cells to the site of Trm activation. Trm can also activate cells of the innate immune system including dendritic cells and natural killer cells that in turn can create an immune environment potentiating graft rejection [31].

Conclusions

In summary, we described that in the absence of systemic lymph nodes, allogeneic hind limb grafts reject in delayed fashion and that splenectomy in the setting of absent lymph nodes further adds to graft survival without eliminating rejection altogether. Absence of allograft, donor-origin, lymph nodes did not contribute to further extension of graft survival, finding that might reflect their regulating role of the immune response. The capacity to isolate these peripheral and central modes of allosensitization will facilitate a reductionist approach to further study primarily vascularized organ allografts.

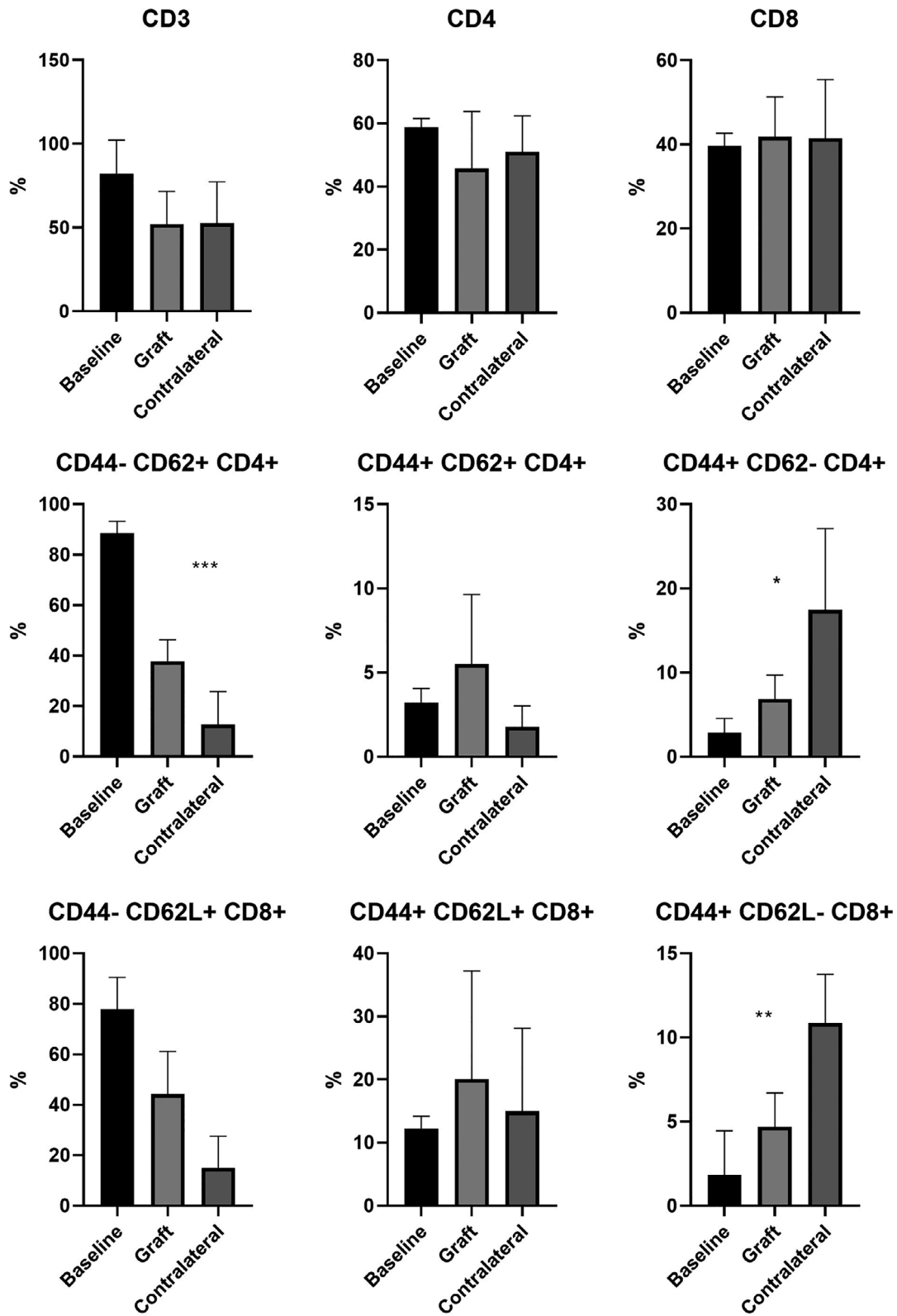


Figure 4 Flow cytometry of femoral nodes in the syngeneic group. There were no differences in the % of CD3, CD4, and CD8 populations in both graft and contralateral (native) nodes. There was a significant decrease in the % of naïve (CD44⁻CD62⁺, $P < 0.01$) and a significant increase in effector memory cells (CD44⁺CD62⁻, $P < 0.05$) in the CD4 population compared to baseline (pretransplant) levels. Similar trends were noted in the CD8 population. No differences were found in the central memory subset (CD44⁺CD62⁺).

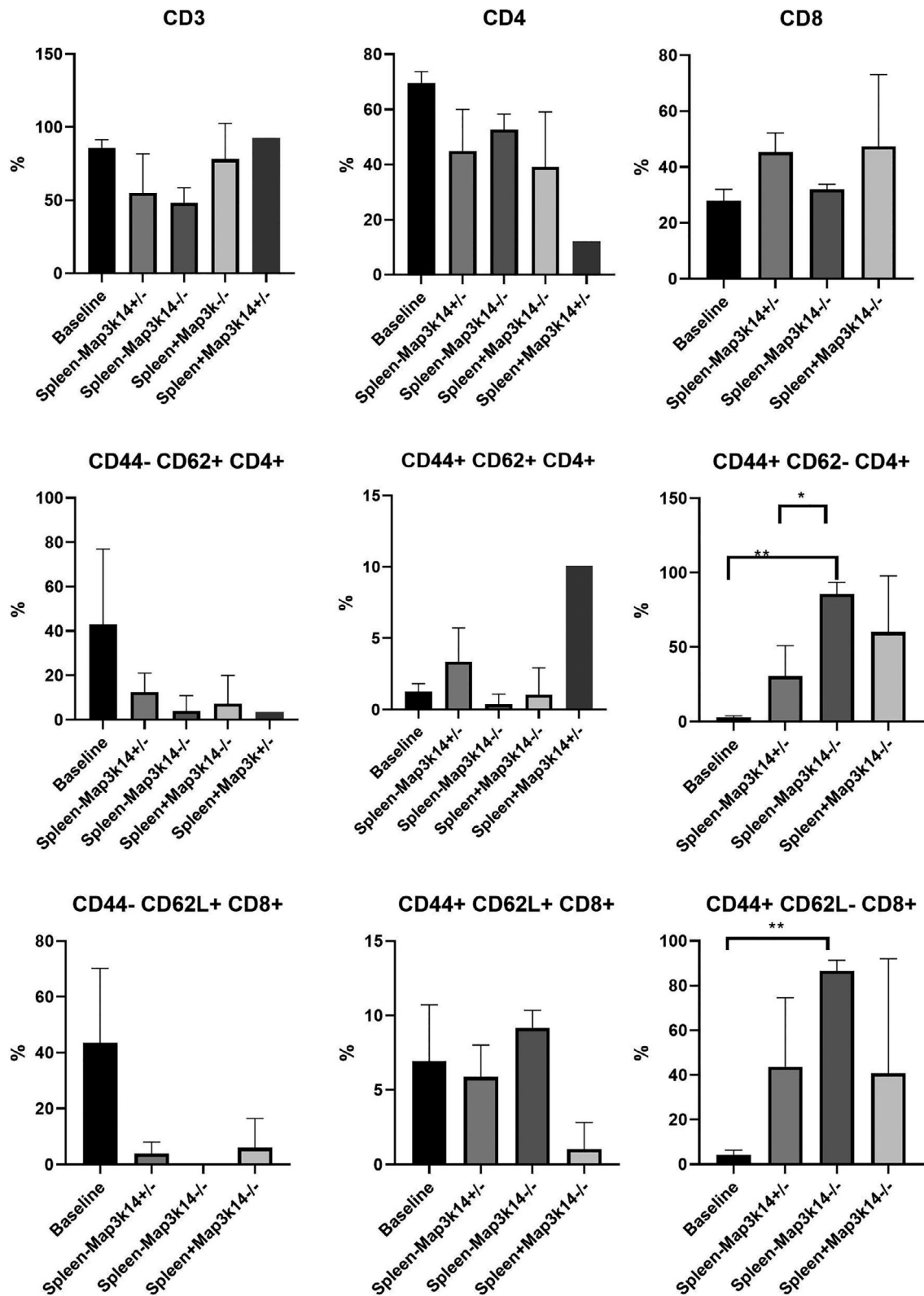


Figure 5 Flow cytometry of femoral nodes in the allogeneic groups. There were no differences in the % of CD3, CD4, and CD8 populations among all groups. There was a decrease in the % of naïve (CD44⁻CD62⁺) and an increase in effector memory cells (CD44⁺CD62⁻) in the CD4 population compared to baseline. These trends were more profound in the Spleen-Map3k14^{-/-} group. Similar trends were noted in the CD8 population.

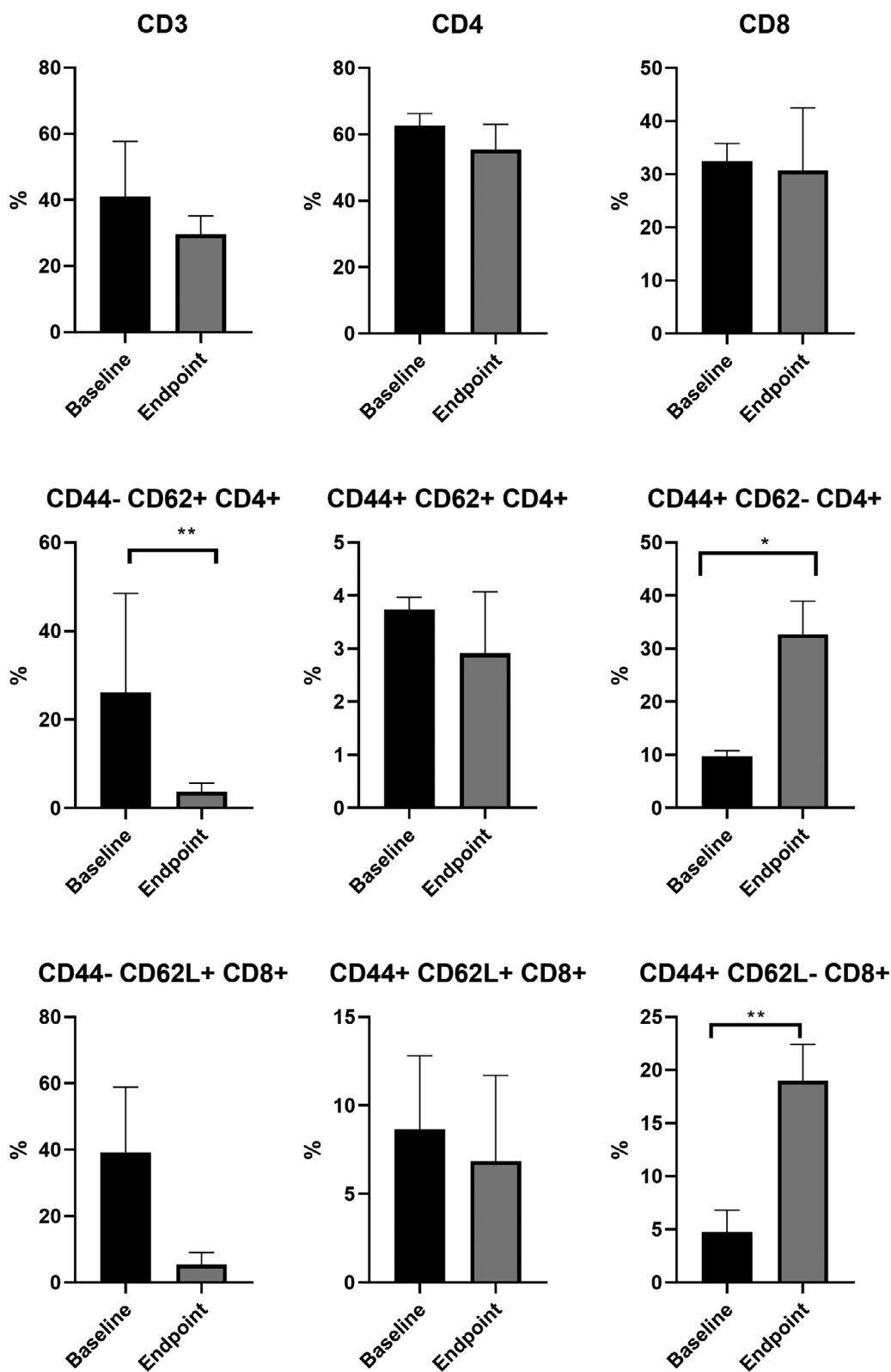


Figure 6 Flow cytometry of spleen in the syngeneic group. There were no differences in the % of CD3, CD4, and CD8 populations among all groups. There was a significant decrease in the % of naïve ($P < 0.01$) and an increase in effector memory cells ($P < 0.05$) in the CD4 subset compared to baseline. Similar trends were noted in the CD8 population.

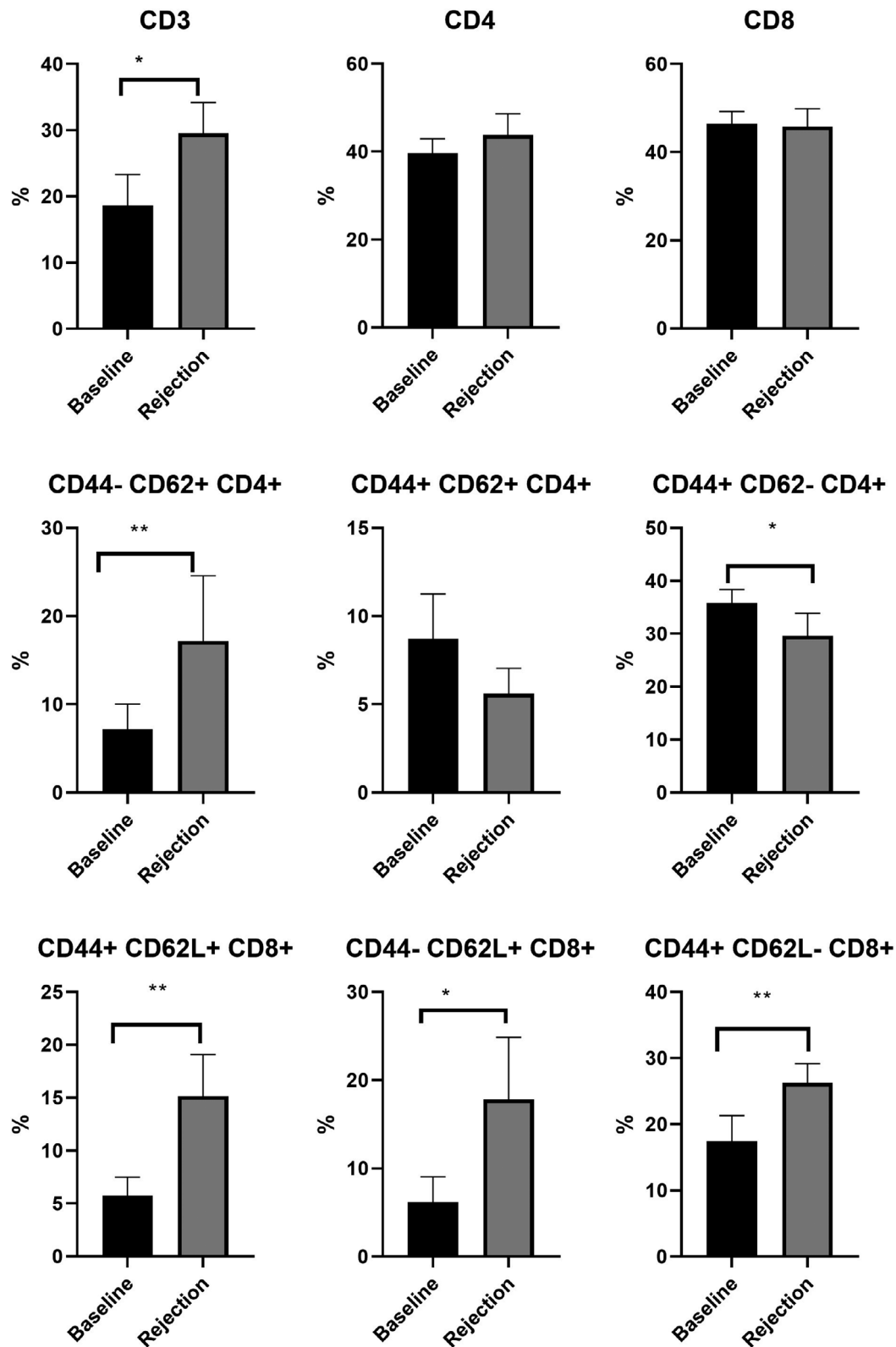


Figure 7 Flow cytometry of spleen in the Map3k14^{+/-} group. There was a significant increase in the % of CD3 cells at the time of rejection compared to baseline. There were no differences in the % of CD4 and CD8 populations. There was a significant increase in the % of naïve ($P < 0.01$) and a decrease in effector memory cells ($P < 0.05$) in the CD4 population compared to baseline. However, in the CD8 population, all CD8 subsets were increased compared to baseline ($P < 0.05$).

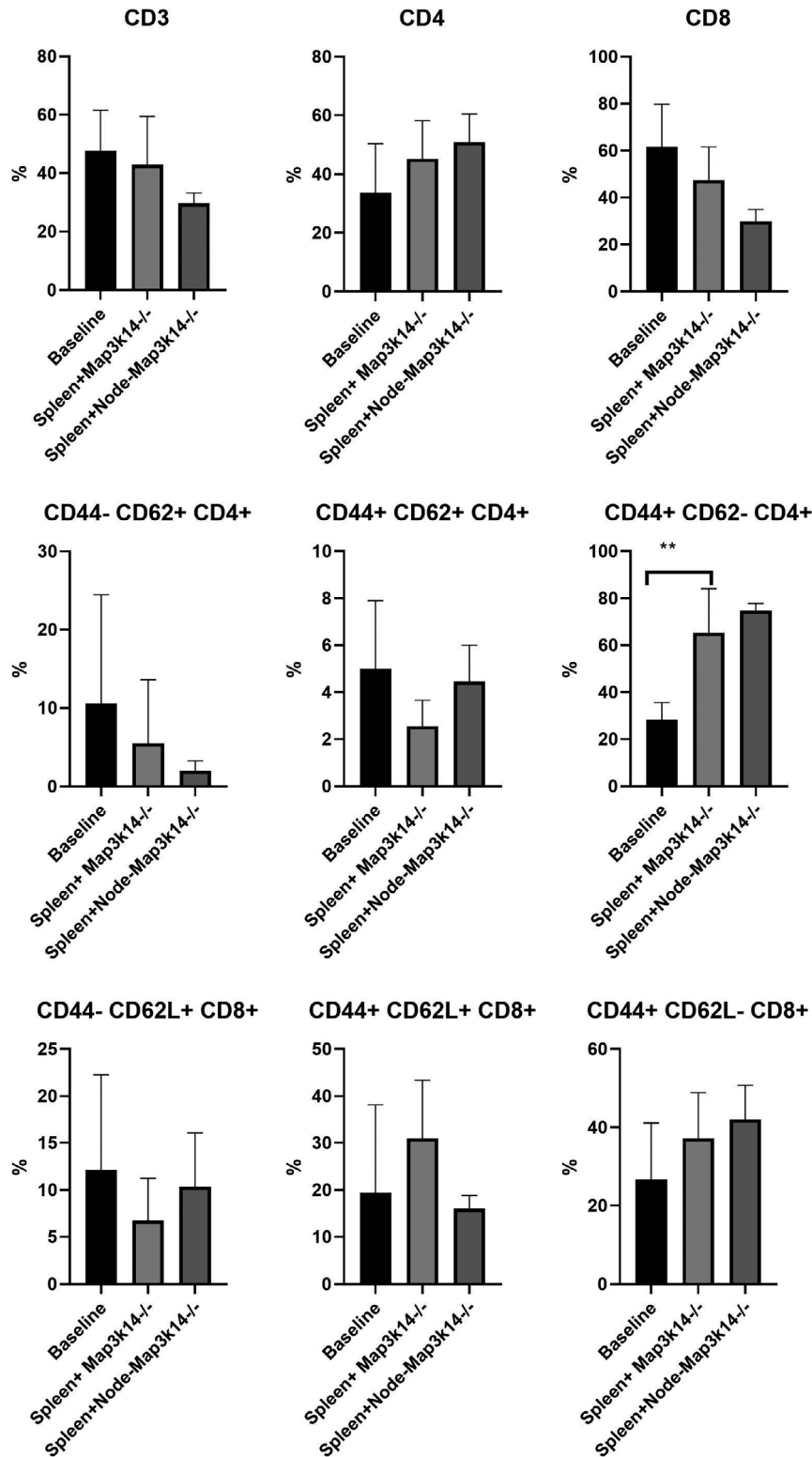


Figure 8 Flow cytometry of spleen in the Map3k14^{-/-} groups. There were no differences in the % of CD3, CD4 and CD8 populations among all groups at the time of rejection compared to baseline. There were no differences in the % of CD4 and CD8 populations. There was a decrease in the % of naïve and an increase in effector memory cells in the CD4 population compared to baseline that was more profound in the Node- group. Similar trends were noted in the CD8 subsets.

Authorship

DM, ADK and LCC: participated in research design. DM, MS, LS, ADK and LCC: participated in the writing of the paper. DM, JW, MAS, MS, LS, WP, ADK and LCC: participated in the performance of the research. MAS, MS and LS: contributed new reagents or analytic tools. DM, LS, ADK and LCC: participated in data analysis.

Funding

Duke Health Scholars Award (LC).

Conflict of interest

The authors have declared no conflicts of interest.

Acknowledgements

This study was funded by the 0 (LC). The authors want to thank the Duke Surgery Core for Microsurgery and Surgical Models in Small Animals and the Substrate

Services Core for Research Support their technical assistance, and Dr. Rebecca Vernon for her contribution to animal care.

SUPPORTING INFORMATION

Additional supporting information may be found online in the Supporting Information section at the end of the article.

Figure S1. Identification of graft nodes (femoral and popliteal) before transplantation with the use of methylene blue foot pad injection (50 μ l).

Figure S2. Gating strategy for flow cytometry analysis.

Figure S3. Clinical presentation (a) and HE staining (b) in a Spleen⁻Map3k14^{-/-} mouse that did not develop any skin graft lesions by day 90 post-transplant.

Figure S4. Flow cytometry of the peripheral blood among Map3k14^{-/-} groups.

Table S1. Identification of graft nodes (femoral and popliteal) before transplantation with the use of methylene blue foot pad injection (50ul).

REFERENCES

- Pomahac B, Becker YT, Cendales L, *et al.* Vascularized composite allotransplantation research: the emerging field. *Am J Transplant* 2012; **12**: 1062.
- Cendales L, Hardy MA. Immunologic considerations in composite tissue transplantation: overview. *Microsurgery* 2000; **20**: 412.
- Giannis D, Moris D, Cendales LC. Costimulation blockade in vascularized composite allotransplantation. *Front Immunol* 2020; **11**: 544186.
- Munding GS, Narushima M, Hui-Chou HG, *et al.* Infrared fluorescence imaging of lymphatic regeneration in nonhuman primate facial vascularized composite allografts. *Ann Plast Surg* 2012; **68**: 314.
- Ng YH, Chalasani G. Role of secondary lymphoid tissues in primary and memory T-cell responses to a transplanted organ. *Transplant Rev* 2010; **24**: 32.
- Lewis SM, Williams A, Eisenbarth SC. Structure and function of the immune system in the spleen. *Sci Immunol* 2019; **4**: eaau6085.
- Pober JS, Merola J, Liu R, Manes TD. Antigen presentation by vascular cells. *Front Immunol* 2017; **8**: 1907.
- Atia A, Moris D, McRae M, *et al.* Th17 cell inhibition in a costimulation blockade-based regimen for vascularized composite allotransplantation using a nonhuman primate model. *Transpl Int* 2020; **33**: 1294.
- Ford ML, Koehn BH, Wagener ME, *et al.* Antigen-specific precursor frequency impacts T cell proliferation, differentiation, and requirement for costimulation. *J Exp Med* 2007; **204**: 299.
- Vernon R, Wang J, Song M, Wilson N, Moris D, Cendales L. Vascularized composite allotransplantation: a functional hind limb model in mice. *J Surg Res* 2020; **250**: 119.
- Eshima K, Misawa K, Ohashi C, Noma H, Iwabuchi K. NF-kappaB-inducing kinase contributes to normal development of cortical thymic epithelial cells: its possible role in shaping a proper T-cell repertoire. *Immunology* 2020; **160**: 198.
- Lacher SM, Thurm C, Distler U, *et al.* NF-kappaB inducing kinase (NIK) is an essential post-transcriptional regulator of T-cell activation affecting F-actin dynamics and TCR signaling. *J Autoimmun* 2018; **94**: 110.
- Miyawaki S, Nakamura Y, Suzuka H, *et al.* A new mutation, aly, that induces a generalized lack of lymph nodes accompanied by immunodeficiency in mice. *Eur J Immunol* 1994; **24**: 429.
- Sallusto F, Geginat J, Lanzavecchia A. Central memory and effector memory T cell subsets: function, generation, and maintenance. *Annu Rev Immunol* 2004; **22**: 745.
- Cendales LC, Kanitakis J, Schneeberger S, *et al.* The Banff 2007 working classification of skin-containing composite tissue allograft pathology. *Am J Transplant* 2008; **8**: 1396.
- Pei J, Li Y, Chen C, *et al.* Inhibition of lymphatic drainage with a self-designed surgical approach prolongs the vascularized skin allograft survival in rats. *Ann Plast Surg* 2018; **80**: 76.
- Rinkinen J, Selley R, Agarwal S, Loder S, Levi B. Skin allograft and vascularized composite allograft: potential for long-term efficacy in the context of lymphatic modulation. *J Burn Care Res* 2014; **35**: 355.
- Larsen CP, Morris PJ, Austyn JM. Migration of dendritic leukocytes from cardiac allografts into host spleens. A novel pathway for initiation of rejection. *J Exp Med* 1990; **171**: 307.

19. Larsen CP, Morris PJ, Austyn JM. Donor dendritic leukocytes migrate from cardiac allografts into recipients' spleens. *Transpl Proc* 1990; **22**: 1943.
20. Lakkis FG, Arakelov A, Konieczny BT, Inoue Y. Immunologic 'ignorance' of vascularized organ transplants in the absence of secondary lymphoid tissue. *Nat Med* 2000; **6**: 686.
21. Tedesco-Silva H, Mourad G, Kahan BD, *et al.* FTY720, a novel immunomodulator: efficacy and safety results from the first phase 2A study in de novo renal transplantation. *Transplantation* 2005; **79**: 1553.
22. Wang J, Dong Y, Sun JZ, *et al.* Donor lymphoid organs are a major site of alloreactive T-cell priming following intestinal transplantation. *Am J Transplant* 2006; **6**: 2563.
23. Gelman AE, Li W, Richardson SB, *et al.* Cutting edge: acute lung allograft rejection is independent of secondary lymphoid organs. *J Immunol* 2009; **182**: 3969.
24. Kant CD, Akiyama Y, Tanaka K, *et al.* Both rejection and tolerance of allografts can occur in the absence of secondary lymphoid tissues. *J Immunol* 2015; **194**: 1364.
25. Neely HR, Flajnik MF. Emergence and evolution of secondary lymphoid organs. *Annu Rev Cell Dev Biol* 2016; **32**: 693.
26. Ranghino A, Segoloni GP, Lasaponara F, Biancone L. Lymphatic disorders after renal transplantation: new insights for an old complication. *Clin Kidney J* 2015; **8**: 615.
27. Mulvihill MS, Samy KP, Gao QA, *et al.* Secondary lymphoid tissue and costimulation-blockade resistant rejection: a nonhuman primate renal transplant study. *Am J Transplant* 2019; **19**: 2350.
28. Freitas AM, Samy KP, Farris AB, *et al.* Studies introducing costimulation blockade for vascularized composite allografts in nonhuman primates. *Am J Transplant* 2015; **15**: 2240.
29. Ruddle NH. High endothelial venules and lymphatic vessels in tertiary lymphoid organs: characteristics, functions, and regulation. *Front Immunol* 2016; **7**: 491.
30. Hautz T, Zelger BG, Nasr IW, *et al.* Lymphoid neogenesis in skin of human hand, nonhuman primate, and rat vascularized composite allografts. *Transpl Int* 2014; **27**: 966.
31. Beura LK, Rosato PC, Masopust D. Implications of resident memory T cells for transplantation. *Am J Transplant* 2017; **17**: 1167.